Case Studies in Thermal Engineering 8 (2016) 128–140

Contents lists available at ScienceDirect

Case Studies in Thermal Engineering

journal homepage: www.elsevier.com/locate/csite

Latent energy storage: Melting process around heating cylinders

T. Kousksou [a,*], M. Mahdaoui [a], M. Hlimi [b], R. El Alaiji [c], T. El Rhafiki [c]

[a] Laboratoire des Sciences de l'Ingénieur Appliquées à la Mécanique et au Génie Electrique (SIAME), Université de Pau et des Pays de l'Adour – IFR – A. Jules Ferry, 64000 Pau, France
[b] École Supérieure de Technologie de Fès, Université Sidi Mohamed Ibn Abdelah, Route d'Imouzzer, BP 2427, Morocco
[c] Ecole Nationale Supérieure d'Arts et Métiers, ENSAM, Marjane II, BP 4024 Meknès Ismailia, Morocco

ARTICLE INFO

Article history:
Received 20 May 2016
Received in revised form
22 June 2016
Accepted 22 June 2016
Available online 23 June 2016

Keywords:
Melting
PCM
Natural convection
Heat storage
Multiple cylinders

ABSTRACT

A physical model to investigate the melting process around a multiple of heating cylinders in the presence of the natural convection has been carried out. A numerical code is developed using an unstructured finite-volume method and an enthalpy porosity technique to solve for natural convection coupled to solid-liquid phase change. It is found that during the melting process around the cylinders, natural convection circulation around each cylinder interacts with the other cylinders to influence the melt shape. In addition to natural convection, the heat source arrangement is an important factor in determining the melt shape.

1. Introduction

Energy sources will play an important role in the world's future given that the global demand for energy is rapidly increasing. It is estimated that the consumption of electrical energy will double in the next 15–20 years [1]. Estimates of the world primary energy consumption are that 80% of the supply is provided by fossil fuels [2]. The primary energy use is estimated to rise between 32% and 84% by 2050 as compared to 2007 [3]. The greenhouse gas (GHG) emissions from electricity generation are approximately 40% of total emissions as most of that industry uses fossil fuels, particularly coal and oil, hence area leading contributor to global energy-related CO_2 emissions [4,5]. The impacts of climate change are now too evident to be disputed. As the Stern Review points out [6], it would be too costly to tackle the challenge of climate change if the world procrastinates in taking actions. Using renewable energy sources seems a promising option; however, there are still some serious concerns about some renewable energy sources and their implementation, e.g. (i) capital cost and (ii) their intermittent nature in power production [7–9].

Among the renewable energy sources, solar power generation undoubtedly offers the most promising and viable option for electricity generation for the present and future. By using adequate equipment sun irradiation energy can be converted into thermal and electrical energy. Depending on the temperature of the working fluid we can differ between the low-temperature ($T < 100\ ^\circ C$), middle-temperature ($100\ ^\circ C < T < 400\ ^\circ C$) and high-temperature solar thermal energy conversion

* Corresponding author.
E-mail address: Tarik.kousksou@univ-pau.fr (T. Kousksou).

http://dx.doi.org/10.1016/j.csite.2016.06.010

Nomenclature

c	specific heat capacity (J kg^{-1} K^{-1})
f	liquid fraction
$\vec{g}$	the acceleration of gravity vector (m s^{-2})
L_F	melting heat (J kg^{-1})
Nu	Nusselt number
p	pressure (Pa)
S	surface (m^2)
T	temperature (°C)
t	time (s)
$\vec{u}$	vitesse vector (m s^{-1})
V	control volume (m^3)
x	coordinate (m)

Greek symbols

$\bar{\bar{\tau}}$	the viscous stress tensor
λ	thermal conductivity (W m^{-1} K^{-1})
Γ	diffusion coefficient
μ	dynamic viscosity (kg m^{-1} s$^{-1)}$
ρ	density (kg m^{-3})
β	the coefficient of volumetric thermal expansion (K^{-1})

Subscripts

i	initial
m	melting
nb	neighboring

(400 °C < T < 4000 °C). For low-temperature solar energy conversion one uses flat collectors with water and air, for middle temperature conversion one uses vacuum collectors and collectors with concentrators, and for high-temperature conversion one uses solar furnaces and concentrating solar power (CSP) plants [10,11].

In order for the renewable energy resources to become completely reliable as primary sources of energy, energy storage is a crucial factor [12,13]. Essentially, energy from these renewable resources must be stored when an excess is produced and then released.

The thermal energy storage (TES) can be defined as the temporary storage of thermal energy at high or low temperatures [14–16]. TES systems have the potential of increasing the effective use of thermal energy equipment and of facilitating large-scale switching. They are normally useful for correcting the mismatch between supply and demand energy [13,17–19].

Certainly, TES is of particular interest and significance in using this essential technique for solar thermal applications such as heating, hot water, cooling, air- conditioning, etc., because of its intermittent nature [20–23]. In these applications, a TES system must be able to retain the energy absorbed for at least a few days in order to supply the energy needed on cloudy days when the energy input is low. One of the thermal energy storage system concepts takes advantage of the latent-heat-of-fusion of phase change material (PCM) to store and recover thermal energy. A latent thermal storage system possesses three major components: (i) a heat storage system that undergoes a solid-to-liquid transformation within the desired operating temperature range, (ii) containment of the storage substance, and (iii) a heat exchanging surface for transferring heat from the source to the storage substance and from the latter to the heat load.

Solid-liquid phase change heat transfer relevant to latent heat-of-fusion energy storage systems has been a subject of many theoretical and experimental studies [24–27]. In this paper, we investigate numerically the heat transfer during the melting process of PCM around a multiple horizontal heat sources (see Fig. 1). This study is motivated by the need to gain improved understanding of heat transfer during the charging phase of TES system which takes advantage of latent heat-of-fusion of PCM. A relevant consideration in such systems is the effective utilization of the PCM by an optimum arrangement of tubes through which the working fluid is circulated. Good heat transfer characteristics between the transport fluid and the PCM for efficient thermal performance of a storage unit are also required [21,28]. Natural convection is also an important process in problems involving melting [29–32], and it is the purpose of this paper to point out some of its characteristics.

2. Mathematical formulation

The general assumptions considered in this work include transient formulation and two dimensional Newtonian incompressible fluid where the natural convection effects are considered. The thermophysical properties of the PCM are assumed to be constant but may be different for the liquid and solid phases. The Boussinesq approximation is valid, i.e., liquid density variations arise only in the buoyancy source term, but are otherwise neglected.

Since the present formulation deals with solutions on unstructured grids, it is essential to represent the conservation laws in their respective integral forms.

$$\int_S \vec{u}.\,\vec{n}\,dS = 0 \tag{1}$$

$$\frac{\partial}{\partial t}\int_V \rho\,\vec{u}\,dV + \int_S \rho\,\vec{u}\,\vec{u}.\,\vec{n}\,dS = -\int_V \vec{\nabla} p\,dV + \int_S \bar{\bar{\tau}}.\,\vec{n}\,dS + \int_V \vec{A}_U dV \tag{2}$$

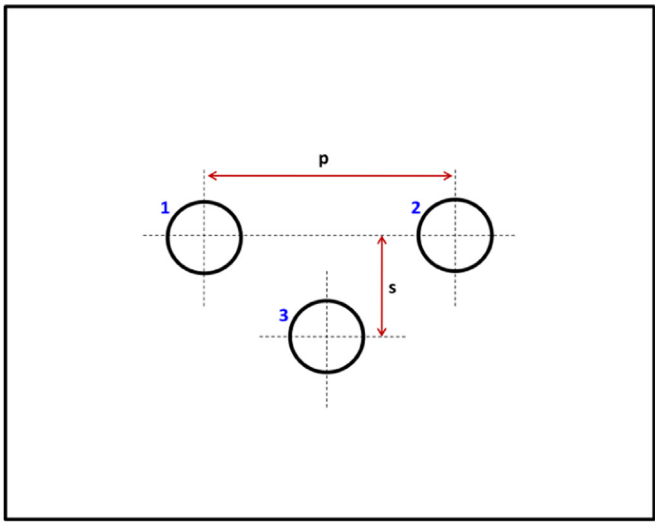

(A)

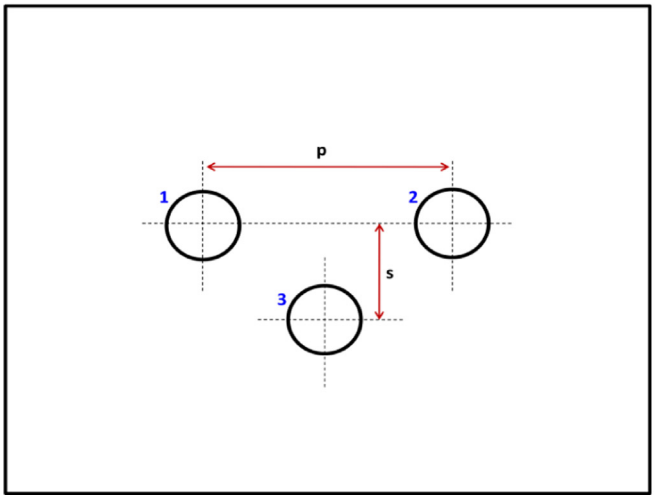

(B)

Fig. 1. Cylindrical heat source arrangements used in tests.

Table 1
Cylindrical heat source arrangements used in tests: D=0.02 m.

Arrangement	Pitch, p	Spacing, s
A_1	3D	D
A_2	3D	1.5D
B_1	3D	D
B_2	3D	1.5D

$$\frac{\partial}{\partial t}\int_V \rho\, c_p T\, dV + \int_S \rho\, c_p T\, \vec{u}.\,\vec{n}\, dS = \int_S \lambda \vec{\nabla} T.\,\vec{n}\, dS + \int_V \rho L_F \frac{\partial f}{\partial t} \tag{3}$$

where $\vec{u}$ is the velocity vector, p the pressure and T the temperature. $\bar{\bar{\tau}}$ is the viscous stress tensor for a Newtonian fluid:

$$\bar{\bar{\tau}} = \mu\left(\bar{\bar{\nabla}} u + \left(\bar{\bar{\nabla}} u\right)^T\right) \tag{4}$$

Table 2
Physical properties of pure Gallium.

Density (liquid)	6093 kg m^{-3}
Reference temperature	29.78 °C
Volumetric thermal expansion coefficient of liquid	1.2 10^{-4} K^{-1}
Thermal conductivity	32 W m^{-1} K^{-1}
Melting temperature (T_m)	29.78 °C
Latent heat of fusion	80,160 J kg^{-1}
Specific heat capacity	381.5 J kg^{-1}
Dynamic viscosity	1.81 10^{-3} kg m^{-1} s^{-1}
Prandtl number	2.16 10^{-2}

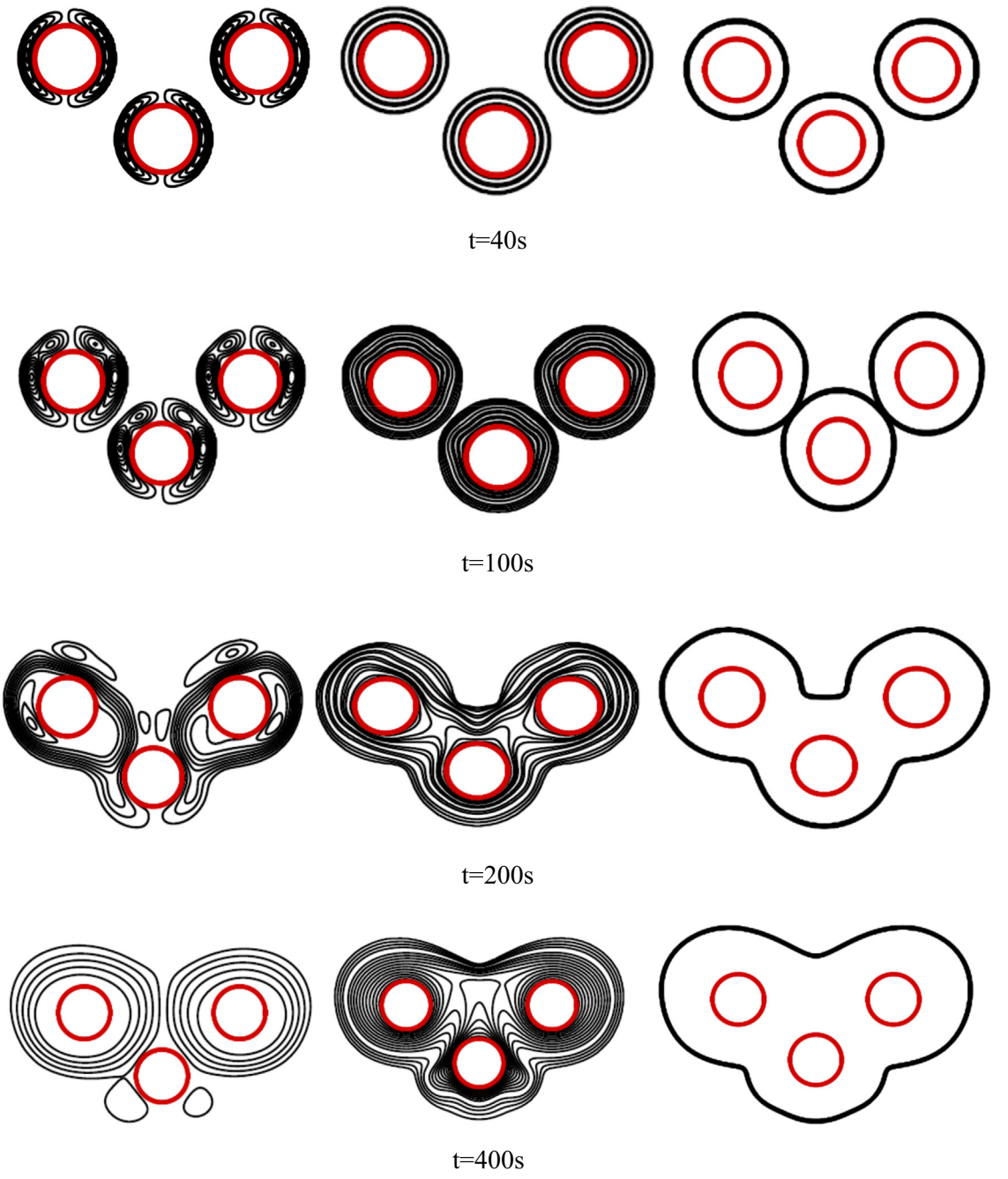

Fig. 2. Stream lines, temperatures contours and interfaces liquid-solid at various times for T_w=311 K (Arrangement A_1).

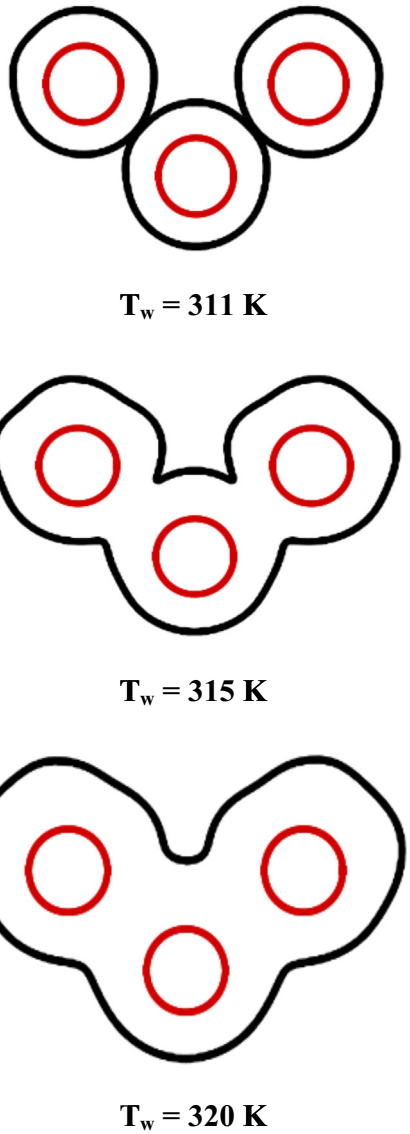

Fig. 3. Interfaces liquid-solid for various wall temperatures at t = 100 s (Arrangement A_1).

The integration occurs over a control volume V surrounded by a surface S, which is oriented by an outward unit normal vector $\vec{n}$. The source term in Eq. (2) contains two parts:

$$\vec{A}_U = \rho\,\beta(T - T_m)\vec{g} + A\,\vec{u} \tag{5}$$

where β is the coefficient of volumetric thermal expansion and $\vec{g}$ the acceleration of gravity vector. The first part of the term source represents the buoyancy forces due to the thermal dilatation. T_m is the melting temperature of the PCM. The last term is added to account for the velocity switch-off required in the solid region. During the solution process of the momentum field, the velocity at the computational cell located in the solid phase should be suppressed while the velocities in the liquid phase remain unaffected. Also, as the solid region melts the mass in the corresponding computational cell should begin to move. The present study adopts a Darcy-like momentum source term to simulate the velocity switch-off [33].

$$A = -\frac{C(1-f)^2}{f^3 + \varepsilon} \tag{6}$$

The constant C has a large value to suppress the velocity at the cell becomes solid and ε is small number used to prevent the division by zero when a cell is fully located in the solid region, namely $f = 0$. In this work, $C = 1 \times 10^{15} kg/m^3 s$ and $\varepsilon = 0.001$ are used.

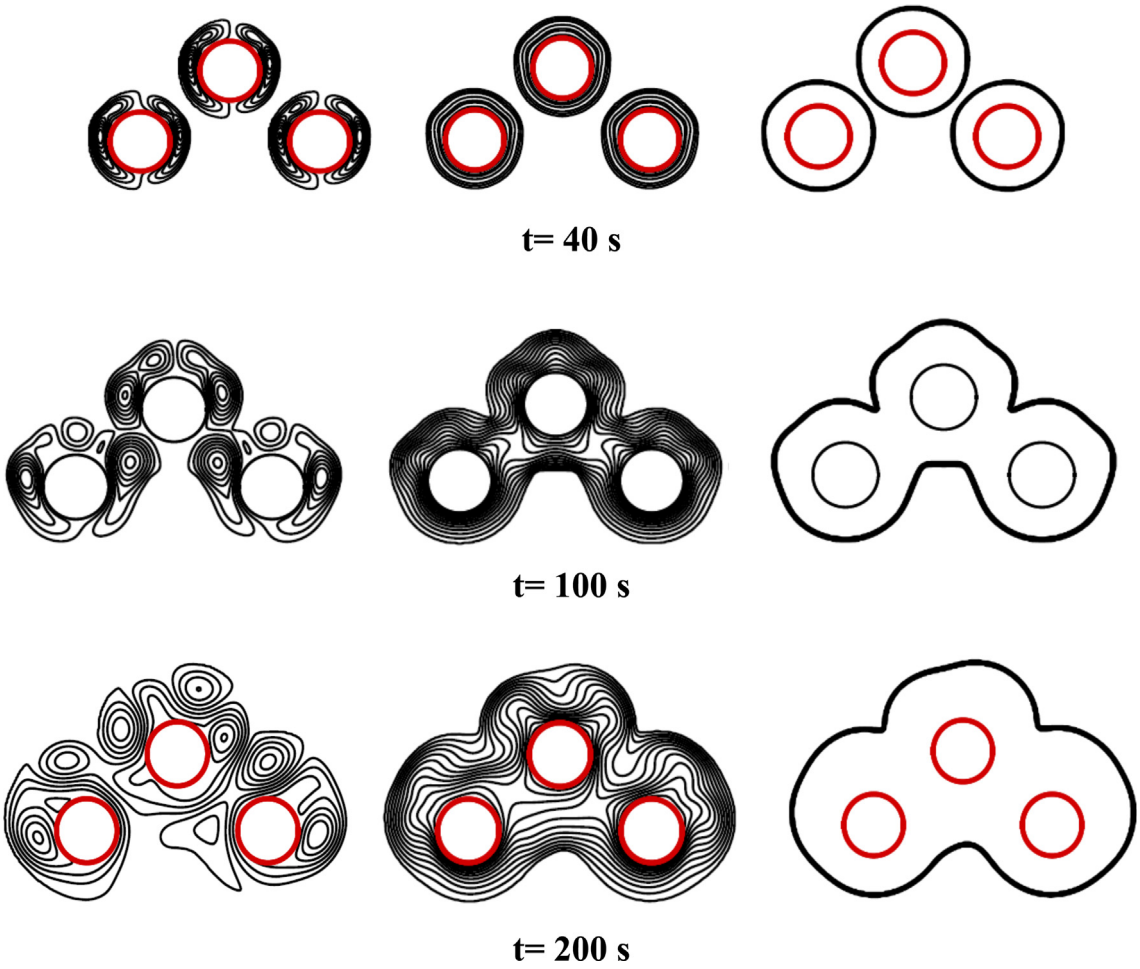

Fig. 4. Stream lines, temperatures contours and interfaces liquid–solid at various times for T_w=315 K (Arrangement B_1).

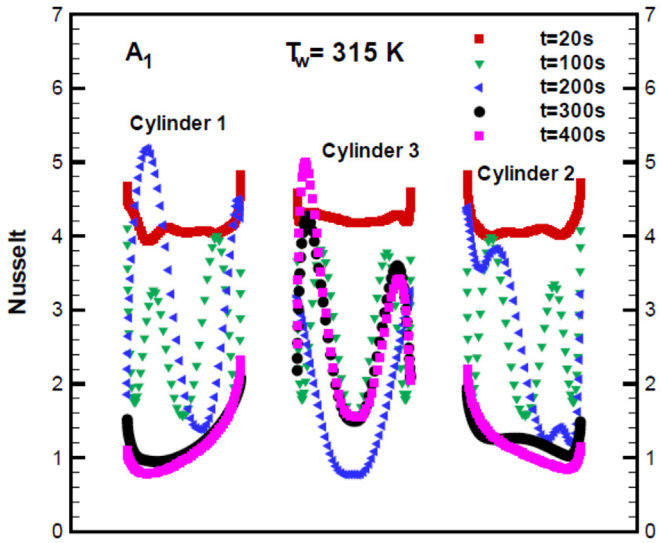

Fig. 5. Nusselt number versus time (Arrangement A_1).

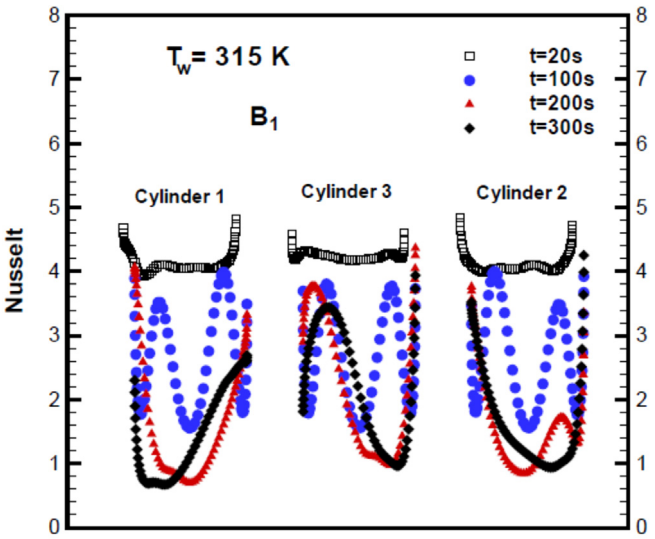

Fig. 6. Nusselt number versus time (Arrangement B_1).

3. Numerical procedure

The conservation Eq. (1)–(3), are solved by implementing them in an in house code. The present code [34,35] has a two dimensional unstructured finite-volume framework that is applied to hybrid meshes. The variables values are stored in cell centers in a collocated arrangement. All the conservation equations have the same general form. By taking into account the shape of control volumes, the representative conservation equation to be discretized may be written as

$$\frac{d}{dt}\int_V \rho\,\phi\,dV + \sum_i \int_{S_j}\left[\rho\,u_i\phi - \Gamma_\phi\frac{\partial\phi}{\partial x_i}\right]dS_i = \int_V S_\phi dV \tag{7}$$

Solidification and melting are generally transient phenomena, where the explicit schemes are too restrictive owing to stability limitations. Hence implicit schemes are often preferred and the simplest choice is the first order Euler scheme. The cell face values, appearing in the convective fluxes, were obtained by blending the upwind differencing scheme (UDS) and the central difference scheme (CDS) using the differed correction approach [36,37]. The coupling of the dependent variables was obtained on the basis of the iterative SIMPLE algorithm developed by Patankar and Spalding [38,39].

Summation of the fluxes through all the faces of a given control volume (CV) results in an algebraic equation which links the value of the dependent variable at the CV center with the neighboring values. The equation may also be written in a conventional manner as

$$A_P\phi_P = \sum_{nb} A_{nb}\phi_{nb} + b_\phi \tag{8}$$

The coefficients A_{nb} contain contributions of the neighboring (nb) CVs, arising out of convection and diffusion fluxes as defined by Eqs. (1)–(3). The central coefficientA_P on the other hand, includes the contributions from all the neighbors and the transient term. In some of the cases, where sources term linearization was applied, it also contained part of the source terms. b_φ contains all the terms those are treated as known (source terms, differed corrections and part of the unsteady term).

The evaluation of the source term in the energy equation has been made using the new source algorithm proposed by Voller [40] where the new value of liquid fraction f at iteration$n$ in cell P is calculated as follows:

$$f_P^{n+1} = f_P^n + \frac{A_P^n\Delta t}{\rho\,L_F V}(T_P - T_m) \tag{9}$$

This update is followed by an overshoot/undershoot correction:

$$f_P^{n+1} = \begin{cases} 0 & if \quad f_P^{n+1} < 0 \\ 1 & if \quad f_P^{n+1} > 1 \end{cases} \tag{10}$$

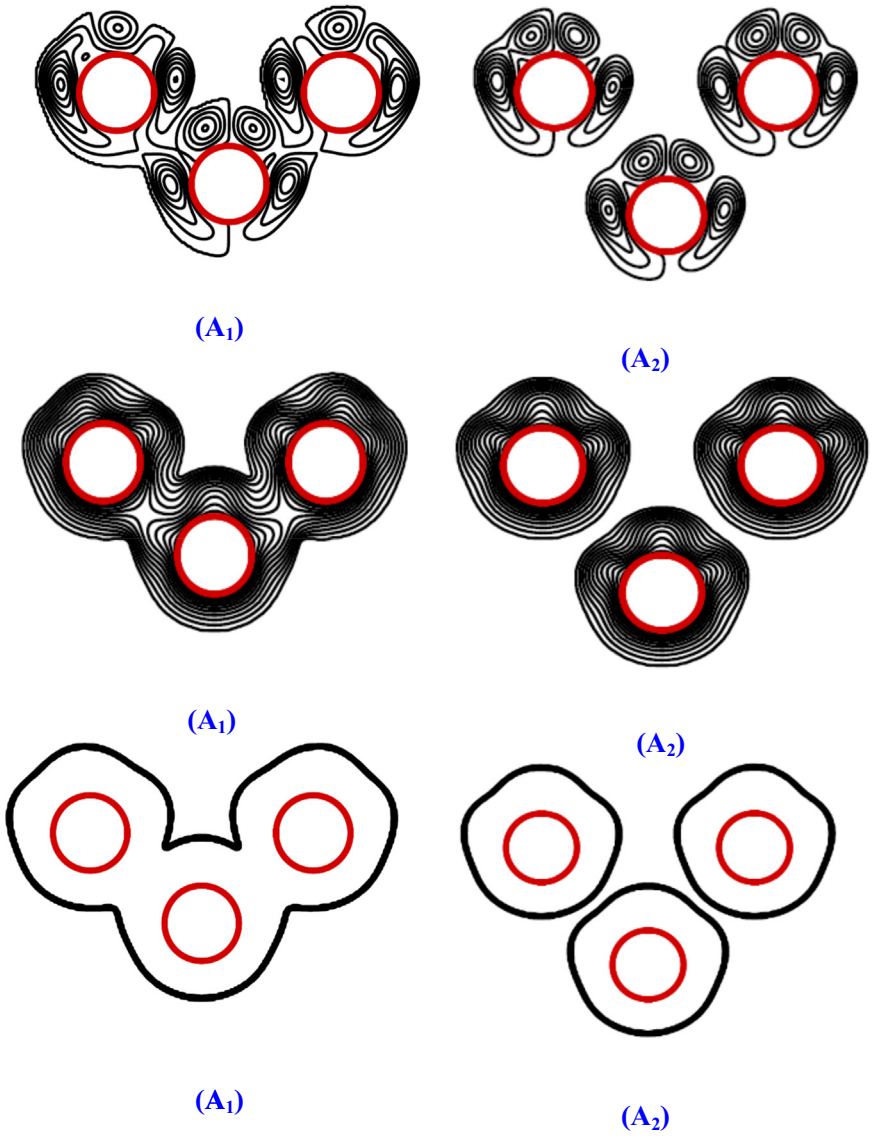

Fig. 7. Stream lines, temperatures contours and interfaces liquid-solid at t = 100 s for arrangement A (T_w = 315 K).

The momentum, pressure correction and temperature are solved sequentially using an ILU-preconditioned GMRES procedure implemented in the IML++ library [41]. All of the computational meshes were generated using the open-source software Gmsh [42].

The numerical procedure to study phase change processes were validated elsewhere and will not presented here [43]. It has seen that the validation of the results obtained with this formulation and the code resulted in excellent agreement with those of the literature [44].

4. Results and discussions

Using the above-described model, simulations were carried out for melting of a PCM around three horizontal cylinder arrangements. Two different arrangements (see Fig. 1) have been considered to examine the effects of natural convection during the melting process on the heat transfer and the melting front shape. The pitch and the spacing used are given in Table 1.

Galium is selected as PCM that its thermophysical properties are taken in Table 2. The solid PCM was subcooled at $T_S = 302K$ where the wall temperature of the inner cylinder is fixed at $T_W > T_m$. Numerical investigations were conducted using 75,000 cells and the time step of 10^{-4} s was found to be sufficient to give accurate results.

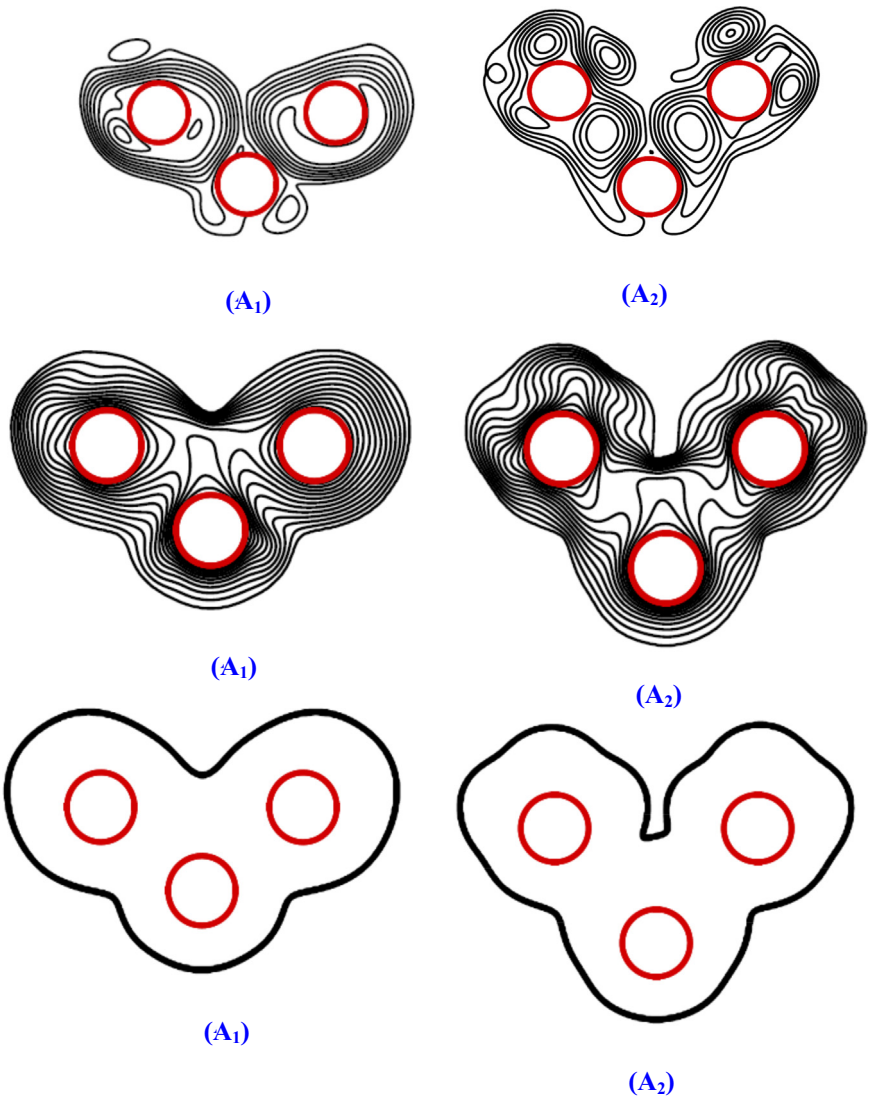

Fig. 8. Stream lines, temperatures contours and interfaces liquid-solid at t=200 s for arrangement A (T_w=315 K).

The influence of the melting process on the streamlines, temperature contours and the solid-liquid interface for various times for arrangement (**A_1**) is illustrated through the result illustrated in Fig. 2. Most of the melting occurs above and to the sides of heat sources with very little below. At early times the liquid is confined between the rigid heated cylinder and a concentric moving solid-liquid interface. Inspection of the plots reveals also that at early times the melt regions are similar in shape and that when heat transfer to the gallium is predominantly by conduction the melt region is symmetrical about the axis of the cylinder. After some time natural convection develops and intensifies, influencing the melt shape in general and the melt region above the cylinders in particular. Natural convection in the melt supports the phase change process as melting continues particularly above the heat source. However, as long as the individual melt regions have not merged to form a common liquid region around the cylinders with a common solid-liquid interface, each melt region develops independently and is not influenced by the presence of other heat source. The strong upward thrust of the melting zone is caused by natural convection. At early stages of natural convection a plume rises from the top of the heated cylinder an at later times circulation conveys the hot liquid to the upper part of the melt zone and in this manner continues to support the upward movement of the solid-liquid interface. As the heating continues and natural convection develops, the annular melt zone becomes increasingly distorted. The increase in the wall temperature can provoke oscillation of the plume above the cylinder (see Fig. 3). As the wall temperature of the cylinders increases the solid above the cylinder melts faster. After the liquid regions around the cylinders form a common boundary, the natural convection about the lower cylinder 3 supports melting in the region between and above cylinders 1 and 2. With increasing the wall temperature, the natural convection

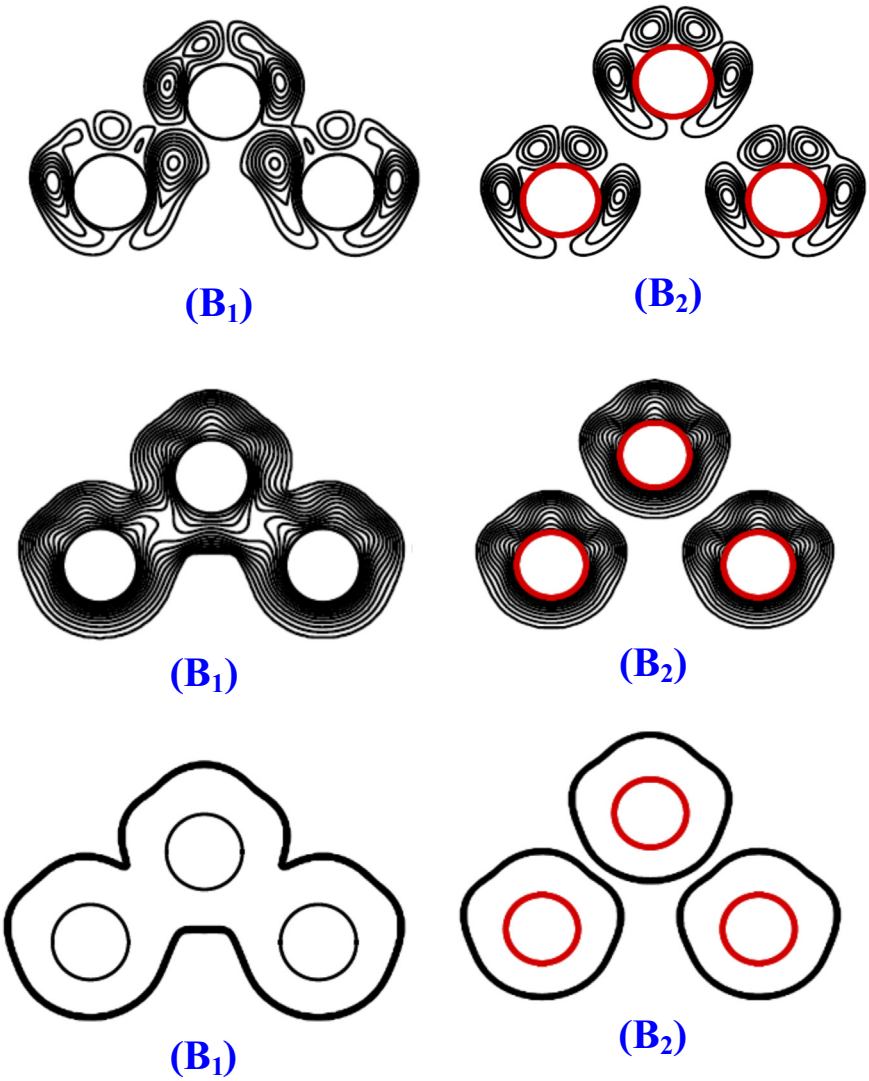

Fig. 9. Stream lines, temperatures contours and interfaces liquid-solid at t = 100 s for arrangement B (T_w = 315 K).

circulation in the liquid becomes more intense and influences the shape of the melt particularly in the region between and above the upper two cylinders (see Fig. 3).

The plumes which rose from the top of the heated cylinders were unstable and affected the shape of the solid-liquid interface. When the circulation was sufficiently intense, the plume above cylinder 3 was influenced by the circulation between cylinders 1 and 2 and originated on the upper part of the cylinder. The plumes of cylinders 1 and 2 produced nonuniform, jagged melting shapes above the upper of two cylinders.

The effect of the melting process on the streamlines, temperature contours and the solid-liquid interface for several times for arrangement (**B_1**) is presented in Fig. 4. The very important role played by natural convection in forming the melt zones is evident from these plots. Most of the melting occurs above and the sides of the heat sources with very little below. Inspection of the plots reveals that at early times the melt regions are still separated. The upward motion of the interface is driven at early times by plume which rises from the top of heated cylinder, and at later times by circulation which conveys the hot liquid to the upper part of the melt regions. It appears that the presence of natural convection reduces the melting below the cylinders compared to that which would occur if heat transfer were by pure conduction.

The local Nusselt number at the hot wall is a good indicator of how convection affects overall conduction around the three cylinders. Figs. 5 and 6 show the evolution of the local Nusselt number at the top part of the three cylinders for several times and for the two arrangements **A_1** and **B_1**. At early times when heat transfer by conduction predominates the local Nusselt for both arrangements A_1 and B_1 is practically constant at the top part of the three cylinders. As melting continues and natural convection develops, the Nusselt number becomes non uniform. The Nusselt number reaches a constant quasi-

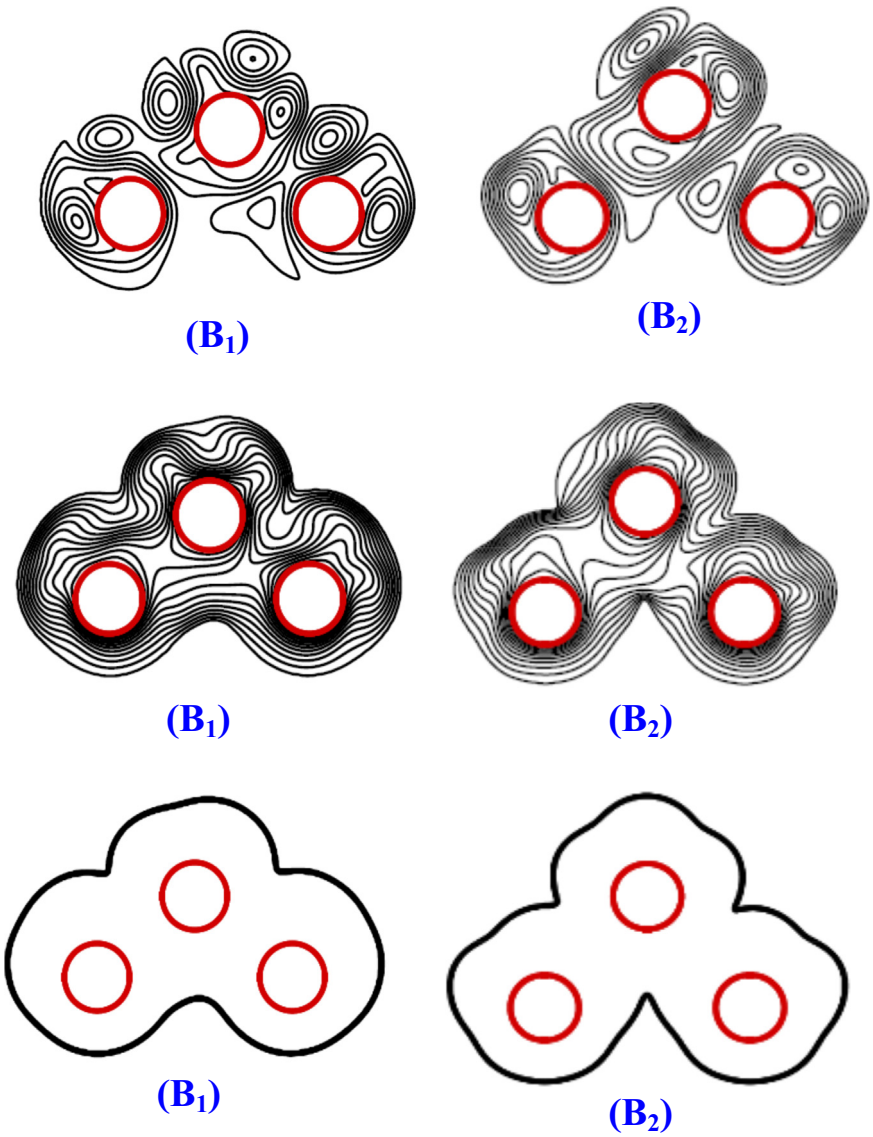

Fig. 10. Stream lines, temperatures contours and interfaces liquid-solid at t=200 s for arrangement B (T_w=315 K).

steady value at large time even though the solid liquid interface continues to move as melting progresses. This suggests that the processes which occur in the neighborhood of the interface do not contribute significantly to the overall thermal resistance to heat transfer. The variation of the local Nusselt at the top part of the cylinder can also be used to detect the oscillation of the plume in the top part of the cylinder which becomes important between 200 s and 300 s

For arrangements **A_1 and B_1** a continuous solid-liquid interface has already been formed while for **A_2** and **B_2** the cylinders still have separate melt zones (see Figs. 7 and 9). This is due to closer spacing of heat sources for arrangements **A_1 and B_1** (see Table 1). For arrangements **A_2** and B_2 the melt zones extend into the vertical and for **A_1 and B_1** into the horizontal directions (see Figs. 8 and 10).

Fig. 11 illustrates the time evolution of the total liquid fraction (ratio of volume of melt to volume cavity) versus time for the four arrangements (A_1, A_2, B_1 and B_2). From the liquid fraction versus time plot, one can get both the rate melting (slope of the tangent line at a given time) and the average melting rate (ratio of current liquid fraction and time). As can be seen, arrangements A_1 and B_1 proved to be more effective in melting the PCM than arrangements A_2 and B_2. This is due to closer spacing of heat sources for arrangements A_1 and B1. We can also note that arrangement B_1 is more effective than arrangement A_1. This is due to the more intense natural convection circulation in the melt for arrangement B_1.

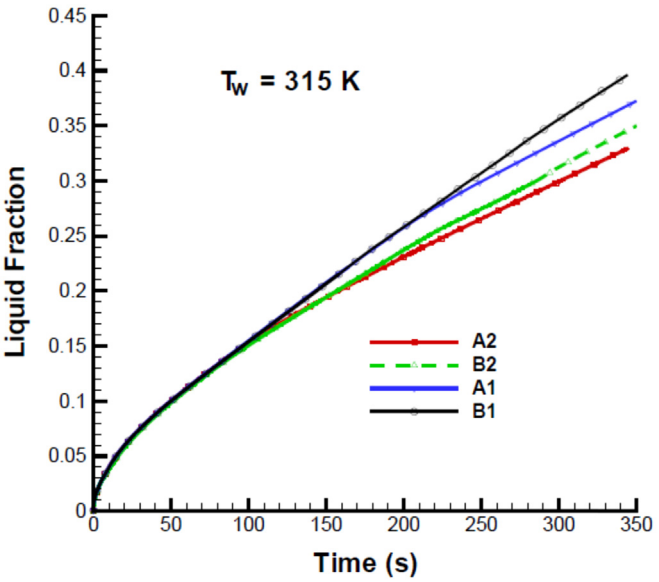

Fig. 11. Liquid fraction versus time for different arrangements.

5. Conclusion

Melting of PCM from multiple cylindrical heat sources has been studied numerically. It is found that after a common solid-liquid interface is formed around the cylinders, natural convection circulation around each cylinder interacts with the other cylinders to influence the melt shape. In addition to natural convection, the heat source arrangement is an important factor in determining the melt shape. For an effective utilization of a PCM in TES system the effect of natural convection and of cylinder arrangement are important and have to be accounted for in the design of such systems.

References

[1] International Energy Agency, World Energy Outlook-2006, IEA, 2007.
[2] International Energy Agency, Energy technology perspectives, Paris, 2010.
[3] D. Barlev, R. Vidu, P. Stroeve, Innovation in concentrated solar power, Sol. Energy Mater. Sol. Cells 95 (2011) 2703–2725.
[4] IEA Statistics: CO_2 emissions from fuel combustion, International Energy Agency (IEA), 2011.
[5] F. Zabihian, A. Fung, Fuel and GHG emission reduction potentials by fuel switching and technology improvement in the Iranian electricity generation sector, Int. J. Eng. 3 (2009) 159–173.
[6] N. Stern, The Economics of Climate Change, American Economic Review 98 (2008)1–37. A recent assessment by the former chief economist of the World Bank.
[7] M.M. Farid, A.M. Khudhair, S.A.K. Razack, S. Al-Hallaj, A review on phase change energy storage: materials and applications, Energy Convers. Manag. 45 (2004) 1597–1615.
[8] M. Beaudin, H. Zareipour, A. Schellenberglabe, W. Rosehart, Energy storage for mitigating the variability of renewable electricity sources: an updated review, Energy, Sustain. Dev. 14 (2010) 302–314.
[9] M. Ban, G. Krajačić, M. Grozdek, T. Ćurko, N. Duić, The role of cool thermal energy storage (CTES) in the integration of renewable energy sources (RES) and peak load reduction, Energy 48 (2012) 108–117.
[10] A. Fernandez-Garcia, E. Zarza, L. Valenzuela, M. Perez, Parabolic-trough solar collectors and their applications, Renew. Sustain. Energy Rev. 7 (2010) 1695–1721.
[11] T. Kousksou, P. Bruel, Encapsulated phase change material under cyclic pulsed heat load, Int. J. Refrig. 33 (2010) 1648–1656.
[12] T. Kousksou, F. Strub, J. Castaing Lasvignottes, A. Jamil, J.P. Bédécarrats, Second law analysis of latent thermal storage for solar system, Sol. Energy Mater. Sol. Cells 91 (2007) 1275–1281.
[13] T. Kousksou, P. Bruel, A. Jamil, T. El Rhafiki, Y. Zeraouli, Energy storage: applications and challenges, Sol. Energy Mater. Sol. Cells 120 (2014) 59–80.
[14] S. Mat, A.A. Al-Abidi, K. Sopian, M.Y. Sulaiman, A.T. Mohammad, Enhance heat transfer for PCM melting in triplex tube with internal-external fins, Energy Convers. Manag. 74 (2013) 223–236.
[15] H. Mehling, L.F. Cabeza, Heat and Cold Storage with PCM, an Up to Date Introduction into Basics and Applications, Springer,, Berlin, Heidelberg, 2008.
[16] B. Zalba, J. MaMarin, L.F. Cabeza, H. Mehling, Review on thermal energy storage with phase change: materials, heat transfer analysis and applications, Appl. Therm. Eng. 23 (2003) 251–283.
[17] A. Sharma, V.V. Tyagi, C.R. Chen, D. Buddhi, Review on thermal energy storage with phase change materials and applications, Renew. Sustain. Energy Rev. 13 (2009) 318–345.
[18] S. Jegadheeswaran, S.D. Pohekar, T. Kousksou, Exergy based performance evaluation of latent heat thermal storage system: a review, Renew. Sustain. Energy Rev. 14 (2010) 2580–2595.
[19] T. Kousksou, T. Elrhafiki, A. Arid, E. Schall, Y. Zeraouli, Power, efficiency and irreversibility analysis of latent energy system, J. Thermophys. Heat Transf. 22 (2008) 234–239.
[20] R. Tamme, U. Taut, C. Streuber, H. Kalfa, Energy storage development for solar thermal processes, Sol. Energy Mater. 24 (1991) 386–396.

[21] K. Nithyanandam, R. Pitchumani, Computational studies on a latent thermal energy storage system with integral heat pipes for concentrating solar power, Appl. Energy 103 (2013) 400–415.
[22] Y.H. Wan, Y.T. Yang, Three-dimensional transient cooling simulations of a portable electronic device using PCM (phase change materials) in multi-fin heat sink, Energy 36 (2011) 5214–5224.
[23] P. Wang, H. Yao, Z. Lan, Z. Peng, Y. Huang, Y. Ding, Numerical investigation of PCM melting process in sleeve tube with internal fins, Energy Convers. Manag. 110 (2016) 428–435.
[24] K.W. Ng, Z.X. Gong, A.S. Mujumdar, Heat transfer in free convection-dominated melting of a phase change material in horizontal annulus, Int. Commun. Heat Mass Transf. 25 (1998) 631–640.
[25] J. Batina, S. Blancher, T. Kouskou, Modelling of a phase change material melting process heated from below using spectral collocation methods, Int. J. Numer. Methods Heat Fluid Flow 24 (2014) 697–734.
[26] A.G. Bathelt, R. Viskanta, Heat transfer at the solid–liquid interface during melting from a horizontal cylinder, Int. J. Heat Mass Transf. 23 (1980) 1493–1503.
[27] J.W. Ramsey, E.M. Sparrow, L.M.C. Varejao, Melting about a horizontal row of heating cylinders, J. Heat Transf. 101 (1979) 732–733.
[28] N.S. Dhaidan, J.M. Khodadadi, Melting and convection of phase change materials in different shape containers: a review, Renew. Sustain. Energy Rev. 43 (2015) 449–477.
[29] M. Lacroix, Numerical simulation of melting and resolidification of a phase change material around two cylindrical heat exchangers, Numer. Heat Transf. Part A 24 (1993) 143–160.
[30] K. El Omari, T. Kousksou, Y. Le Guer, Impact of shape of container on natural convection and melting inside enclosures used for passive cooling of electronic devices, Appl. Therm. Eng. 31 (2011) 3022–3035.
[31] A. Arid, T. Kousksou, S. Jegadheeswaran, A. Jamil, Y. Zeraouli, Numerical simulation of ice melting near the density inversion point under periodic thermal boundary conditions, Fluid Dyn. Mater. Process. 305 (2012) 1–19.
[32] T. Kousksou, A. Arid, J. Majid, Y. Zeraouli, Numerical modeling of double-diffusive convection in ice slurry storage tank, Int. J. Refrig. 33 (2010) 1550–1558.
[33] S. Kim, M.C. Kim, B. Lee, Numerical analysis of convection driven melting and solidification in a rectangular enclosure, J. Ind. Eng. Chem. 8 (2002) 185–190.
[34] T. Kousksou, M. Mahdaoui, A. Ahmed, A. Ait Msaad, Melting over a wavy surface in a rectangular cavity heated from below, Energy 64 (2014) 212–219.
[35] M. Mahdaoui, T. Kousksou, S. Blancher, A. Ait Msaad, T. El Rhafiki, M. Mouqallid, A numerical analysis of solid–liquid phase change heat transfer around a horizontal cylinder, Appl. Math. Model. 38 (2014) 1101–1110.
[36] P.K. Khosla, S. Rubin, A diagonally dominant second-order accurate implicit scheme, Comput. Fluids 2 (1974) 207.
[37] S. Jana, S. Ray, F. Durst, A numerical method to compute solidification and melting processes, Appl. Math. Model. 31 (2007) 93–119.
[38] S.V. Patankar, Numerical Heat Transfer and Fluid Flow. Hemisphere, Washington DC, 1980.
[39] S.V. Patankar, D.B. Spalding, A calculation of heat, mass and momentum transfer in three dimensional parabolic flows, Int. J. Heat Mass Transf. 15 (1972) 1787–1806.
[40] V. Voller, Fast implicit finite-difference method for the analysis of phase change problems, Numer. Heat Transf. Part B – Fundam. 17 (1990) 155–169.
[41] J. Dongarra, A. Lumsdaine, R. Pozo, K. Remington, A sparse matrix library in C++ for high performance architectures, in: Proceedings of the Second Object Oriented Numerics Conference, 1994, pp. 214–218.
[42] C. Geuzaine, J.F. Remacle, Gmsh: a three dimensional finite element mesh generator with built in pre and post processing facilities, Int. J. Numer. Methods Eng. 79 (2009) 1309–1331.
[43] T. Kousksou, M. Mahdaoui, A. Ahmed, J. Batina, Numerical simulation of PCM melting over a wavy surface, Int. J. Numer. Methods Heat Fluid Flow 24 (2014) 1660–1678.
[44] Z.X. Gong, A.S. Mujumdar, Flow and heat transfer convection-dominated melting in a rectangular cavity heat from below, Int. J. Heat Mass Transf. 41 (1998) 2573–2580.